Bortezomib (Velcade) Induces p27Kip1 Expression through S-Phase Kinase Protein 2 Degradation in Colorectal Cancer

Shahab Uddin,[1] Maqbool Ahmed,[1] Prashant Bavi,[1] Raafat El-Sayed,[2] Nasser Al-Sanea,[3] Alaa AbdulJabbar,[3] Luai H. Ashari,[3] Samar Alhomoud,[3] Fouad Al-Dayel,[4] Azhar R. Hussain,[1] and Khawla S. Al-Kuraya[1]

[1]Department of Human Cancer Genomic Research, Research Center; [2]Department of Comparative Medicine; [3]Colorectal Unit, Department of Surgery; and [4]Department of Pathology, King Faisal Specialist Hospital and Research Center, Riyadh, Saudi Arabia

Abstract

S-phase kinase protein 2 (SKP2), an F-box protein, targets cell cycle regulators including cycle-dependent kinase inhibitor p27Kip1 via ubiquitin-mediated degradation. SKP2 is frequently overexpressed in a variety of cancers. We investigated the role of SKP2 and its ubiquitin-proteasome pathway in colorectal carcinoma using a panel of cell lines, clinical samples, and the NUDE mouse model. Using immunohistochemical analysis on a large tissue microarray of 448 samples, an inverse association of SKP2 expression with p27Kip1 protein levels was seen. A colorectal cancer (CRC) subset with high level of SKP2 and low level of p27Kip1 showed a decreased overall survival ($P = 0.0057$). Treatment of CRC cell lines with bortezomib or expression of small interfering RNA of SKP2 causes down-regulation of SKP2 and accumulation of p27Kip1. Furthermore, treatment of CRC cells with bortezomib causes apoptosis by involving the mitochondrial pathway and activation of caspases. In addition, treatment of CRC cells with bortezomib down-regulated the expression of XIAP, cIAP1, and survivin. Finally, treatment of CRC cell line xenografts with bortezomib resulted in growth inhibition of tumors in NUDE mice via down-regulation of SKP2 and accumulation of p27Kip1. Altogether, our results suggest that SKP2 and the ubiquitin-proteasome pathway may be potential targets for therapeutic intervention for treatment of CRC. [Cancer Res 2008;68(9):3379–88]

Introduction

Colorectal cancer (CRC) is still a cause of high morbidity and mortality rates. Significant improvements have been made in the management of this disease mainly through the introduction of adjuvant chemotherapy agents like flurouracil and oxaliplatin (1). More recently, advances in the understanding of tumor biology have led to the development of targeted therapies (2), allowing progress in the treatment of CRC (3).

The proteasome is an intracellular multicatalytic complex, which together with the two regulators, PA28 (also called proteasome 11S) and PA700 (also called proteasome 19S), forms the 26S proteasome (4, 5). This constitutes the ubiquitin-proteasome system and regulates a number of intracellular proteins that govern cell cycle tumor, growth, and survival by degrading a number of different polypeptides important for cell cycle progression and apoptosis (6–8). The main rate-limiting regulator for p27Kip1 degradation has been recently identified as an SCF-type ubiquitin ligase complex that contains S-phase kinase protein 2 (SKP2) as the specific substrate recognition subunit (9–11). SKP2 specifically binds p27Kip1 and targets it for degradation by the ubiquitin proteolytic system. Recently, it has been shown that overexpression of SKP2 in mantle cell lymphoma decreased the p27Kip1 expression level, whereas inhibition of SKP2 by small interfering RNA (siRNA) increased p27Kip1 and p21waf1 levels (9–12). The important role of SKP2 in controlling p27Kip1 levels have been reported in a number of human cancer, including colorectal, breast, prostate, and oral squamous cell carcinomas (13–15).

The main mechanism of action of antineoplastic agents is their ability to induce apoptosis. Evidence is mounting to indicate that proteasome inhibitors, such as the peptide aldehyde PSI, selectively inhibit the chymotrypsin-like activity of the proteasome and suppress the proliferation of human cancer cells by causing apoptosis and/or cell cycle arrest (16–19). The proteasome inhibitor bortezomib (Velcade) has been approved by the Food and Drug Administration for the treatment of multiple myeloma and mantle cell lymphoma patients who had received at least one prior therapy and many clinical trials are ongoing to examine the efficacy of bortezomib for the treatment of other malignancies (20).

In this study, we first show, using immunohistochemical analysis on a large tissue microarray of 448 samples, that low expression of p27Kip1 and high expression of SKP2 can identify a clinically aggressive subgroup of CRC. We then show that bortezomib treatment of CRC cell lines can interfere with SKP2-mediated p27Kip1 turnover by stabilizing or up-regulating the expression of p27Kip1 and increase the degradation of SKP2 protein *in vitro* and *in vivo*. Furthermore, CRC cells treated with this specific proteasome inhibitor, bortezomib, show cell growth arrest and apoptosis via activation of the caspase cascade and disruption of the mitochondrial equilibrium. Finally, our data show that the growth of CRC cell line xenografts is inhibited by bortezomib treatment due to down-regulation of SKP-2 and up-regulation of p27Kip1. Altogether, these results suggest that proteasome inhibitors may have a great utility in the treatment of CRC.

Materials and Methods

Cell culture. CRC cell lines Colo320, HCT15, and SW480 cells were cultured in RPMI 1640 supplemented with 10% (v/v) fetal bovine serum, 100 units/mL penicillin, and 100 units/mL streptomycin at 37°C in humidified atmosphere containing 5% CO_2. All experiments were performed in RPMI 1640 containing 5% serum.

Note: Supplementary data for this article are available at Cancer Research Online (http://cancerres.aacrjournals.org/).

Requests for reprints: Khawla S. Al-Kuraya, Department of Human Cancer Genomic Research, King Fahad National Center for Children's Cancer and Research, King Faisal Specialist Hospital and Research Cancer, MBC 98-16, P.O. Box 3354, Riyadh 11211, Saudi Arabia. Phone: 966-1-205-5167; Fax: 966-1-205-5170; E-mail: kkuraya@kfshrc.edu.sa.

doi:10.1158/0008-5472.CAN-07-6109

Reagents and antibodies. Bortezomib (Velcade) was a gift from Millenium Pharmaceuticals, Inc. MG132 was purchased from Calbiochem. Antibodies against cleaved caspase-3 and BID antibodies were purchased from Cell Signaling Technologies. Cytochrome *c*, β-actin, caspase-3 and poly(ADP)ribose polymerase (PARP) antibodies were purchased from Santa Cruz Biotechnology, Inc. XIAP, cIAP1, and caspase-8 antibodies were purchased from R&D. Annexin V was purchased from Molecular Probes. Apoptotic DNA-ladder kit was obtained from Roche.

***In vivo* tumor xenograft studies.** Six-week-old NUDE mice were obtained from The Jackson Laboratory and maintained in a pathogen-free animal facility at least 1 wk before use. All animal studies were done in accordance with institutional guidelines. For xenograft study, mice were inoculated s.c. into the right abdominal quadrant with 5 million Colo320 cells in 200 μL PBS. After 1 wk, mice were randomly assigned into two groups receiving either bortezomib or 0.9% saline. Treatment with bortezomib (1 mg/kg) was given i.p. twice weekly. The control group received the vehicle alone at the same schedule. The body weight of each mouse was monitored weekly and tumor volume was measured as described previously (21). After 4 wk of treatment, mice were sacrificed and individual tumors are weighed then snap-frozen in liquid nitrogen for storage.

3-(4,5-Dimethylthiazol-2-yl)-2,5-diphenyltetrazolium bromide assays. Cells (10^4) were incubated in triplicate in a 96-well plate in the presence or absence of indicated test doses of bortezomib in a final volume of 0.20 mL for 24 h. The ability of bortezomib to suppress cell growth was determined by 3-(4,5-dimethylthiazol-2-yl)-2,5-diphenyltetrazolium bromide (MTT) cell proliferation assays, as previously described (22). Replicates of three wells for each dosage, including vehicle control, were analyzed for each experiment.

DNA laddering. DNA laddering assay was performed as described earlier (23). Briefly, cells (2×10^6) were treated with and without bortezomib for 24 h. The cells were then harvested and resuspended in 200 μL 1× PBS. Then, 200 μL lysis buffer containing 6 mol/L guanidine HCl, 10 mmol/L urea, 10 mmol/L Tris-HCl, and 20% Triton X (v/v; pH 4.4), were added to the cells and incubated for 10 min at room temperature. Isopropanol (100 μL) was added and shaken for 30 s on a vortex. Then, samples were passed through a filter and spun at 4,500 × *g* for 1 min, and the supernatant was discarded. The pellets were washed thrice with wash buffer containing 20 mmol/L NaCl, 2 mmol/L Tris-HCl, and 80% ethanol. The pellets were then transferred into a new 1.5-mL tube and eluted with 200 μL prewarmed elution buffer. After measuring the DNA, 2 μg DNA were electrophoresed on a 1.5% agarose gel containing ethidium bromide at 75 V for 2 h and visualized using a UV light source.

Annexin V/propidium iodide dual staining. Colorectal carcinoma cell lines were treated with the indicated concentrations of bortezomib. The cells were harvested and the percentage of cells undergoing apoptosis was measured by flow cytometry after staining with fluorescein-conjugated Annexin V and propidium iodide (Molecular Probes) as previously described (23).

Gene silencing using siRNA. SKP2 siRNA and scrambled control siRNA were purchased from Qiagen. For transient expression, cell lines were transfected by using Lipofectamine 2000 reagent (Invitrogen) according to the manufacturer's instructions. After incubating the cells for 6 h, the lipid and siRNA complex was removed and fresh growth medium was added. Cells were lysed 48 h after transfection and specific protein levels were determined by Western blot analysis with specific antibodies against the targeted proteins and actin as a loading control.

Cell lysis and immunoblotting. Cells were treated with proteasome inhibitor as described in the legends and lysed as previously described (24). Proteins (15–20 μg) were separated by SDS-PAGE and transferred to polyvinylidene difluoride (PVDF) membrane (Immobilon, Millipore). Immunoblotting was done with different antibodies and visualized by the enhanced chemiluminescence (Amersham) method.

Measurement of mitochondrial membrane potential. Cells were treated with bortezomib for 48 h, washed twice with PBS, and suspended in mitochondrial incubation buffer. JC1 was added to a final concentration of 10 μmol/L and cells were incubated at 37°C in dark for 15 min. Cells were then washed twice with PBS and resuspended in 500 μL of mitochondrial incubation buffer and mitochondrial membrane potential (% of green and red aggregates) was determined by flow cytometry as described previously (25).

Assays for cytochrome *c* release. The release of cytochrome *c* from the mitochondria was assayed as described earlier (25). Briefly, cells were treated with and without proteasome inhibitor as described in figure legends, harvested, and resuspended in hypotonic buffer. Cells were homogenized, and cytosolic and mitochondrial fractions were isolated by differential centrifugation. Twenty to 25 μg of protein from cytosolic and mitochondrial fractions of each sample were analyzed by immunoblotting using an anti–cytochrome *c* antibody.

Patient selection and tissue microarray construction. Four hundred forty-eight patients with CRC diagnosed between 1990 and 2006 were selected from King Faisal Specialist Hospital and Research Center. All samples were analyzed in a tissue microarray format. Tissue microarray construction was performed as described earlier (26). Briefly, tissue cylinders with a diameter of 0.6 mm were punched from representative tumor regions of each donor tissue block and brought into recipient paraffin block using a homemade semiautomatic robotic precision instrument. An overview of CRC tissue microarray section is shown in Fig. 1*B*. Three 0.6-mm cores of CRC were arrayed from each case. Clinical and histologic data were available for all these patients. The Colorectal Unit, Department of Surgery, King Faisal Specialist Hospital and Research Center provided long-term follow-up data for these patients. The institutional review board of the King Faisal Specialist Hospital and Research Center approved the study.

Immunohistochemistry. Immunohistochemical studies on formalin-fixed, paraffin-embedded tissue sections were performed as described in earlier studies (27). Tissue microarray slides were processed and stained manually. The streptavidin-biotin peroxidase technique with diaminobenzidine as chromogen was applied. For antigen retrieval, Dako Target Retrieval Solution (pH 9.0) was used, and the slides were microwaved at 750 W for 5 min and then at 250 W for 30 min. The sections were incubated overnight with SKP2 (monoclonal clone 1G12E9, 1:100; Invitrogen), p27Kip1 (monoclonal clone 57, 1:300; Invitrogen), and Ki-67 (monoclonal, clone MIB1, 1:50; Dako), and the Dako Envision Plus System kit was used as the secondary detection system with 3,3′-diaminobenzidine as chromogen. All slides were counterstained with hematoxylin, dehydrated, cleared, and coverslipped with Permount. Grading of nuclear protein staining was based on proportion or percentage of cell nuclei staining and was semiquantified as high or low. Nuclear protein expression of epithelial cells only was scored as high if 50% or more of the nuclei were stained or low if <50% were stained, as has been reported previously (28). Intensity of staining can vary between cases due to different tissue preservation, and, therefore, was not included as a variable in the final scoring.

Statistics. The software used for statistical analysis was Statview 5.0 (SAS Institute, Inc.). The correlation of coefficients between pairs of variables was performed using Pearson's correlation. Survival curves were constructed by the Kaplan-Meier method and multivariate analysis by Cox regression; *P* values <0.05 were considered significant. Two-sided tests were used throughout the analyses.

Results

Overexpression of proteasomal protein SKP2 is inversely associated with p27Kip1 in CRC. Levels of SKP2 and p27Kip1 were examined by immunohistochemistry in a series of 448 colorectal adenocarcinomas. A typical case, shown in Fig. 1*A*, illustrates the decrease in nuclear staining of p27Kip1, increased levels of SKP2 and Ki-67 in tumor sample compared with low SKP2, and Ki-67 and high p27Kip1 expression in another CRC tumor sample. Loss of p27Kip1 expression was seen in 61.8% (243 of 393) and SKP2 overexpression was seen in 27.6% (112 of 406) of the CRC cases. Representative information was available in 393 of 448 spots for p27Kip1 and 406 of 448 spots for SKP2 expression. Expression of

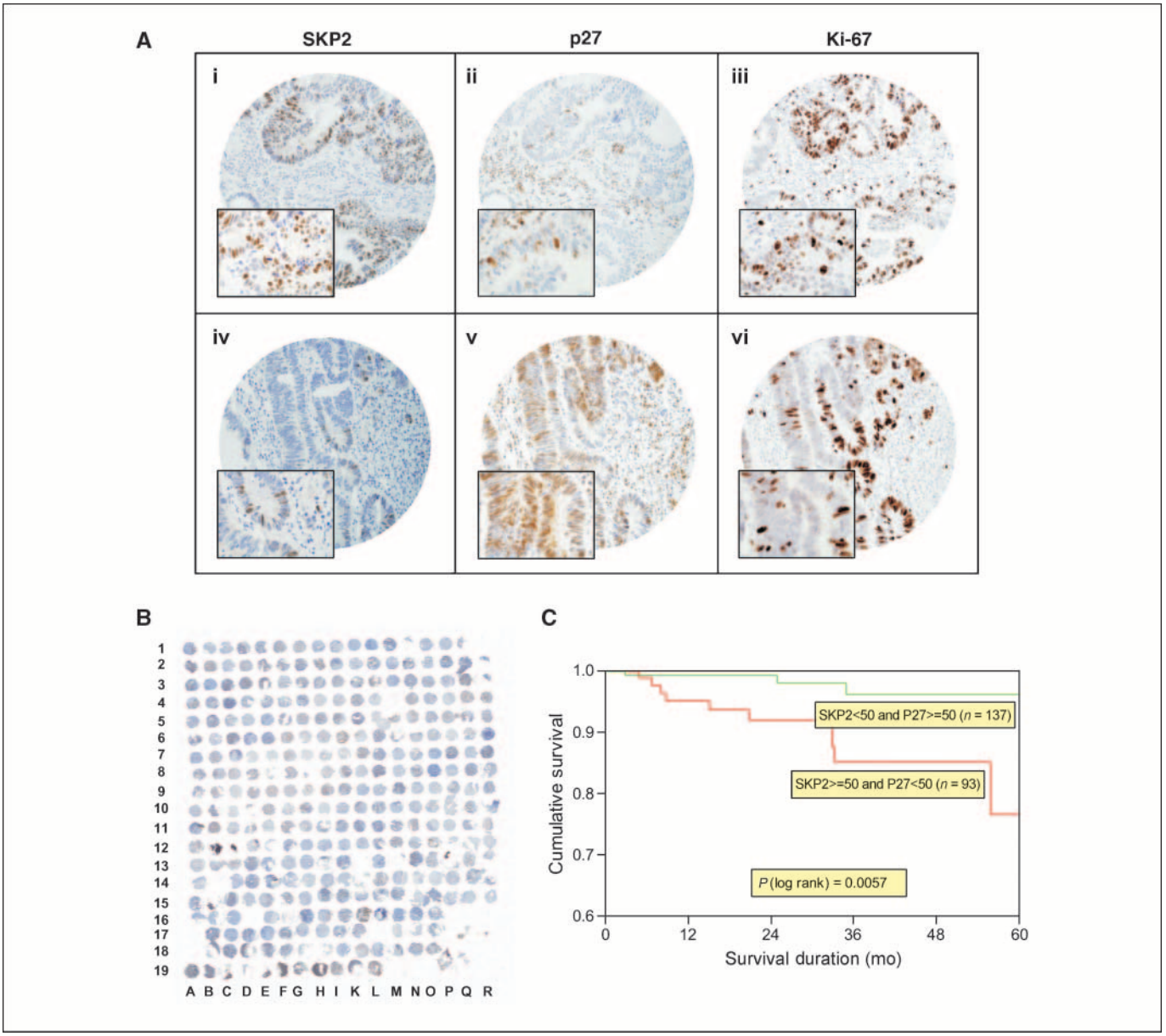

Figure 1. Tissue microarray–based expression analysis of SKP2, p27Kip1, and Ki-67 in CRC. *A,* representative tissue microarray spots demonstrating immunohistochemical staining of colorectal carcinoma. Tumor cells of a colorectal carcinoma exhibiting (*i*) SKP2 overexpression, (*ii*) loss of p27Kip1 expression, and (*iii*) overexpression of proliferative marker Ki-67. Spot of another colorectal carcinoma exhibiting (*iv*) normal expression of p27Kip1, (*v*) low SKP2, and (*vi*) low levels of Ki-67. Original magnification, ×400; *inset,* high-power magnification, ×1,000. *B,* an overview of CRC tissue microarray section stained for SKP2. *C,* the association between SKP2 and p27Kip1 expression groups and overall survival. Analyses were constructed with the Kaplan-Meier method. Overall survival was analyzed by stratifying the patients in two groups: normal SKP2/normal p27 group versus Skp2 overexpression and low p27Kip1 expression. *n,* number of patients.

SKP2 protein was inversely related to p27Kip1 levels ($P < 0.0001$), similar to previous findings (28). SKP2 and p27Kip1 expressions were not associated with patients' age or gender. In addition, neither SKP2 nor p27Kip1 expression was associated with disease stage at presentation. Thus, the expression of these proteins was not significantly different between early disease (stages I and II) and advanced disease (stages III and IV). We further stratified all our CRC cases into two groups depending on the presence of SKP2 expression and p27Kip1 expression status: normal SKP2/normal p27Kip1 group ($n = 137$) and CRC with SKP2 overexpression and low p27Kip1 expression ($n = 93$). The clinicopathologic and the immunohistochemical analyses of the above subset of patients are summarized in Table 1. Such stratification showed significant association of SKP2 overexpression/loss of p27Kip1 CRC expression group with nodal metastasis ($P = 0.0147$) and overexpression of proliferative marker Ki-67 ($P < 0.0001$). Poorly differentiated tumors showed a trend toward higher SKP2 and low p27Kip1 levels compared with well-differentiated tumors ($P = 0.0625$). Furthermore, such stratification showed a significant correlation with overall survival ($P = 0.0057$) and remained significant even in multivariate analysis that included American Joint Committee on Cancer (AJCC) stage and the above-mentioned two groups (Fig. 1*C*). The relative risk for death was 2.4 for the CRC group with SKP2 overexpression and loss of p27Kip1 expression (95% confidence interval, 1.3-5.1; $P = 0.0029$) and 2.5 for AJCC stage group III and IV (95% confidence interval, 1.3-6.4, $P = 0.0040$).

Table 1. Correlation between normal SKP2/normal p27Kip1 versus SKP2 overexpression and low p27Kip1 groups and clinicopathologic features

	n (%)	SKP2 ≥50 and P27 <50, *n* (%)	SPK2 <50 and P27 ≥50, *n* (%)	*P*
Total number of cases	230	93 (40.4)	137 (59.6)	
Age (y)				
≤50	72 (31.3)	35 (48.6)	37 (51.4)	0.0894
>50	158 (68.7)	58 (36.7)	100 (63.3)	
Gender				
Male	127 (55.2)	57 (44.9)	70 (55.1)	0.1261
Female	103 (44.8)	36 (34.9)	67 (65.1)	
Tumor site				
Left colon	199 (86.5)	77 (38.7)	122 (61.3)	0.1765
Right colon	31 (13.5)	16 (51.6)	15 (48.4)	
Histologic type				
Adenocarcinoma	207 (90.0)	81 (39.1)	126 (60.9)	0.2309
Mucinous carcinoma	23 (10.0)	12 (52.2)	11 (47.8)	
Tumor stage*				
I-II	103 (47.3)	44 (42.3)	59 (57.7)	0.6896
III-IV	116 (52.7)	46 (39.7)	70 (60.3)	
pT*				
T_1	9 (4.1)	4 (44.4)	5 (55.6)	0.2353
T_2	42 (19.2)	22 (52.4)	20 (47.6)	
T_3	161 (73.5)	59 (36.6)	102 (63.4)	
T_4	7 (3.2)	4 (57.1)	3 (42.9)	
pN*				
N_0	109 (50.0)	46 (42.2)	63 (57.8)	0.0147
N_1	70 (32.1)	20 (28.6)	50 (71.4)	
N_2	39 (17.9)	22 (56.4)	17 (43.6)	
pM*				
M_0	200 (89.7)	80 (40.0)	120 (60.0)	0.4723
M_1	23 (10.3)	11 (47.8)	12 (52.2)	
Differentiation				
Well	15 (6.5)	6 (40.0)	9 (60.0)	0.0625
Moderate	181 (78.7)	67 (37.0)	114 (63.0)	
Poor	34 (14.8)	20 (58.8)	14 (41.2)	
Ki67 †				
≥50	199 (88.0)	90 (45.2)	109 (54.8)	<0.0001
<50	27 (12.0)	1 (3.7)	26 (96.3)	

*Tumor stage, pT, pN, and pM data were not available in some cases.
†Ki-67 staining was seen in 226 cases; 4 cases were not evaluable for Ki-67 staining.

Proteasomal inhibition induces G_2-M cell cycle arrest and caspase-mediated apoptosis in CRC cell lines. We used a panel of CRC cell lines to determine whether inhibition of proteasome pathways by specific inhibitor leads to growth inhibition of these cancer cell lines. CRC cells were treated with various doses of bortezomib for 48 hours and cell proliferation was determined by MTT assays. As shown in Fig. 2*A*, bortezomib caused a dose-dependent growth inhibition in all the cell lines.

To test whether the reduced growth of CRC cell lines by proteasome inhibition is associated with cell cycle dysregulation, Colo320 cells were treated with various doses of bortezomib and the cell cycle status was analyzed by flow cytometry after staining with propidium iodide. As shown in Fig. 2*B*, after 24 hours of treatment with bortezomib, the percentage of cells in the G_0-G_1 phase was reduced to >50% compared with control, with the treated cells accumulating in the G_2-M phase, suggesting that proteasome inhibition induces cell cycle arrest rather than apoptosis after 24 hours of treatment. To confirm these findings, we analyzed cells after 24-hour treatment with bortezomib with Annexin V/propidium iodide dual staining and we were not able to detect appreciable amount of apoptosis when compared with the untreated control sample (data not shown). However, after 48 hours of treatment with different doses of bortezomib, we detected a shift of cells to the sub-G_1 phase compared with the control sample. The sub-G_1 population of cells increased from 1.52% in the untreated control sample to 26.99% after 50 nmol/L treatment, 26.43% after 100 nmol/L treatment, and 29.36% after 500 nmol/L treatment in Colo320 cells. This increase in the sub-G_1 population was accompanied by a dose-dependent decrease in the percentage of cells in the G_2-M phase. It has been reported that cells with these features are dying of apoptosis (22, 23).

To further confirm that this increase in the sub-G_1 is indeed apoptosis, CRC cell lines were treated with various doses of bortezomib for 48 hours and the cells were stained with FITC-conjugated Annexin V and propidium iodide to assess apoptosis and IC_{50} of CRC cell lines were obtained (Supplementary Fig. S1).

As shown in Fig. 2*C*, there was a dose-dependent increase in the apoptotic cells in the Colo320 cell line as seen by an increase of cells in the upper right quadrant depicting apoptotic cells. The same data were obtained for other cell lines after 48 hours of treatment (HCT-15 and SW-480). One additional method, which is the hallmark of apoptosis, DNA laddering after 48 hours of treatment with various doses of bortezomib, as shown in Fig. 2*D*, confirmed that the cells are actually dying of apoptosis.

Progression through the phases of cell cycle is regulated by periodic activation of several cyclin-dependent kinases (CDK) whose levels are controlled through ubiquitination and proteasomal degradation (29–31). In particular, levels of CDK inhibitors (CDKI) p27Kip1 have been previously shown to be dysregulated following proteasomal inhibition (32–35). There are a number of studies that show SKP2 playing an essential role in degradation of p27Kip1 (9–11). In view of these findings, we sought to determine whether bortezomib-induced apoptosis is due to degradation of SKP2. CRC cell lines were treated with 100 and 500 nmol/L bortezomib for 48 hours. Cells were lysed and proteins were separated on SDS-PAGE and immunoblotted with SKP2. As shown in Fig. 3*A*, bortezomib treatment caused down-regulation of SKP2 in all three cell lines and up-regulation of p27Kip1. LOVO and HCT-116 CRC cell line (Supplementary Fig. S2) showed similar response after bortezomib treatment. A strong inverse relation was found between SKP2 and p27Kip1 after bortezomib treatment. Similar results were obtained with MG132, another inhibitor of proteasome. Bortezomib treatment of DLD-1 CRC cell line failed to induce apoptosis, and no effect was seen on the expression of SKP2 and p27kip1 (Supplementary Fig. S2), suggesting that bortezomib-mediated down-regulation of SKP2 is an important mechanism to induce apoptosis in CRC cell line via up-regulation of p27Kip1. To provide direct evidence whether down-regulation of SKP2 up-regulates p27Kip1, we attempted to inhibit SKP2 expression in Colo320 and HCT-15 cells by the siRNA strategy. For this purpose,

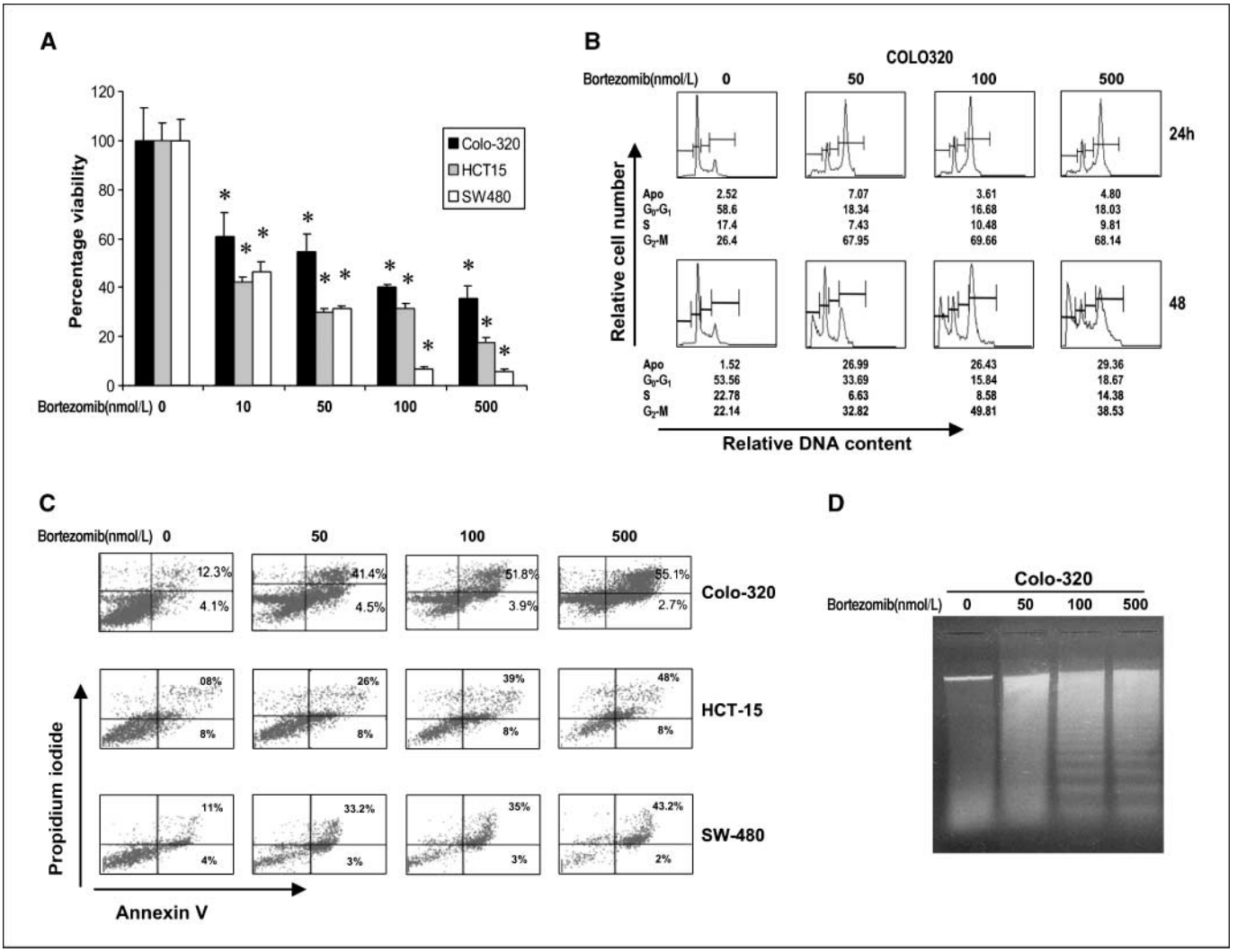

Figure 2. *A,* bortezomib inhibits the proliferation of colorectal carcinoma cells. Colo320, HCT-15, and SW480 cells were incubated with 10, 50, 100, and 500 nmol/L bortezomib for 48 h. Cell proliferation assays were performed using MTT as described in Materials and Methods. *Columns,* mean of three independent experiments with replicates of six wells for all the doses and vehicle control for each experiment; *bars,* SD. *, $P < 0.001$, statistically significant (Student's *t* test). *B,* bortezomib treatment initially causes G_2-M arrest at 24-h treatment leading to accumulation of Apo fraction of cell cycle in CRC cells after 48 h. Colo320 and HCT-15 cells were treated with 50, 100, and 500 nmol/L bortezomib for 48 h. Thereafter, the cells were washed, fixed, and stained with propidium iodide, and analyzed for DNA content by flow cytometry as described in Materials and Methods. *C,* bortezomib-induced apoptosis detected by Annexin V/propidium iodide dual staining. Colo320, HCT-15, and SW480 cells were treated with various doses of bortezomib (as indicated) for 48 h and cells were subsequently stained with fluorescein-conjugated Annexin V and propidium iodide. *D,* Colo320 cells were treated with bortezomib as indicated for 48 h, and DNA was extracted and separated by electrophoresis on 1.5% agarose gel.

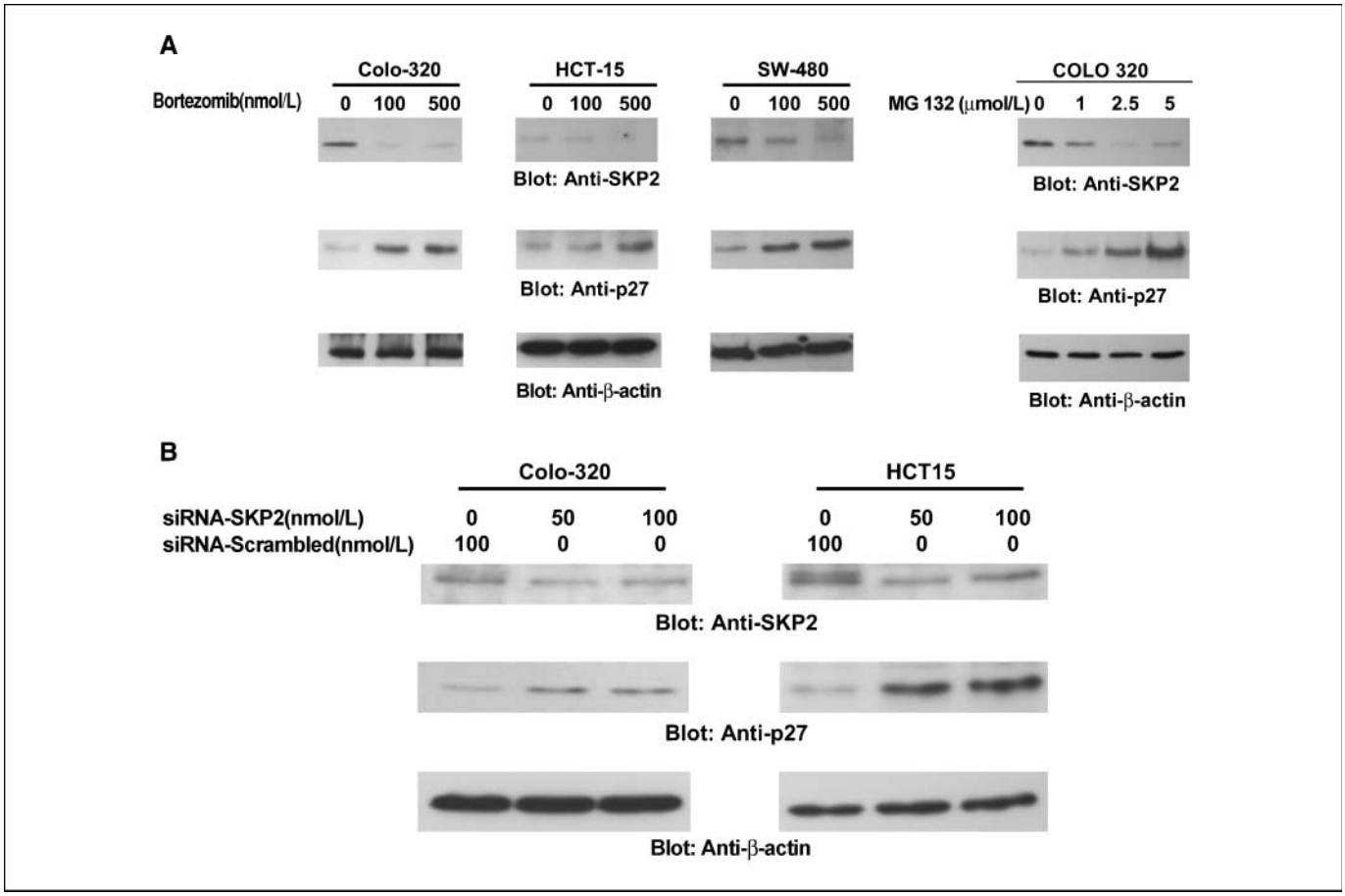

Figure 3. Down-regulation of SKP2 pathway by proteasome inhibition causes accumulation of ubiquitinated proteins and induced level of p27Kip1. *A,* bortezomib treatment down-regulated expression of SKP2 and increased level of p27Kip1. Colo320, HCT-15, and SW-480 cells were treated with and without 100 and 500 nmol/L bortezomib for 48 h. Colo320 cells were also treated with MG132, another inhibitor of proteasome, with indicated doses. After cell lysis, equal amounts of proteins were separated by SDS-PAGE, transferred to Immobilon membrane, and immunoblotted with antibodies against SKP2, p27Kip1, and β actin as indicated. *B,* SKP2 siRNA expression down-regulates SKP2 and accumulated p27Kip1. Colo320 and HCT-15 cells were transfected with scrambled siRNA (100 nmol/L) and SKP2 siRNA (50 and 100 nmol/L) with Lipofectamine as described in Materials and Methods. After 48 h of transfection, cells were lysed and equal amounts of proteins were separated by SDS-PAGE, transferred to Immobilon membrane, and immunoblotted with antibodies against SKP2, P27Kip1, and β actin as indicated.

SKP2 activity was blocked by expression using siRNA against SKP2. As expected in Fig. 3*B*, transfection of siRNA against SKP2 resulted in SKP2 protein depletion as well as concomitant accumulation of p27Kip1 in colon cell lines. Finally, when CRC cells were treated with lower doses of bortezomib (25 and 50 nmol/L) in combination with 0.1 and 0.5 μmol/L 5-fluorouracil, it induced an appreciable amount of apoptosis (Supplementary Fig. S3*A* and S3*B*) and caused down-regulation of SKP-2 leading to accumulation of p27kip1 (data not shown). These results suggest that proteasome inhibition in CRC cell lines stabilized p27Kip1 via down-regulation of SKP2.

The apoptotic signaling cascade starts with activation of caspase-8 and truncation of BID that translocates to the mitochondrial membrane, allowing activation of proapoptotic proteins and release of cytochrome *c*. Therefore, we sought to determine whether down-regulation of SKP2 signaling involves the mitochondria. Activated caspase-8 is capable of cleaving caspase-3 either directly or by digesting BID to its active form (tBID), which leads to the release of cytochrome *c* from the mitochondria. Bortezomib treatment resulted in activation of caspase-8 leading to truncation of BID in Colo320 and SW-480 cells (Supplementary Fig. S4*A*) as inferred by the decreased intensity of the full-length BID band. We then tested the effect of bortezomib on the mitochondrial membrane potentials in these cells. Cells were treated with bortezomib for 48 hours and labeled with JC1 dye and the mitochondrial membrane potential was measured by flow cytometry. As shown in Supplementary Fig. S4*B*, inhibition of proteasome resulted in loss of mitochondrial membrane potential in CRC cells as measured by JC1 stained green fluorescence depicting apoptotic cells. We then studied cytochrome *c* release from the mitochondria in cells treated for 48 hours with bortezomib. Cytochrome *c* was released to the cytosol after bortezomib treatment in Colo320 cells (Supplementary Fig. S4*C*). On the other hand, the level of cytochrome *c* decreased in mitochondrial fraction of Colo320 cells. These results suggest that inhibition of proteasome pathways disrupts the mitochondrial membrane potential leading to the release of cytochrome *c* to the cytosol. We then sought to determine whether bortezomib-induced release of cytochrome *c* is capable of activation of caspase-9, caspase-3, and PARP. Figure 4*A* shows that bortezomib treatment resulted in the activation of caspase-9, caspase-3, and cleavage of PARP in Colo320 and SW-480 cells. These results are consistent with the data on cytochrome *c* release and indicate that activation of effectors caspases participate in bortezomib-induced apoptosis in CRC cells. In addition, pretreatment of Colo320 cells with

80 μmol/L z-VAD-fmk, a universal inhibitor of caspases, abrogated apoptosis and prevented apoptosis and caspase-3 and PARP activation induced by bortezomib (Fig. 4*B* and *C*), clearly indicating that caspases play a critical role in bortezomib-induced apoptosis in colon cancer cells.

Inhibitors of apoptosis proteins (IAP) have been shown to have direct effects on caspase-9 and caspase-3 (36). We therefore also examined whether bortezomib induces cell death by modulating the expression of IAP family members that ultimately determine the cell response to apoptotic stimuli. Colo320 cell line was treated with 100 and 500 nmol/L bortezomib for 48 hours and expression of cIAP1, XIAP and survivin were determined using Western blotting. As shown in Fig. 4*D*, bortezomib treatment caused down-regulation of cIAP1, XIAP, and survivin. These results implicate that these survival proteins may be modulated by proteasomal inhibition for the survival of CRC cells.

***In vivo* activity of proteasome inhibitor bortezomib against CRC xenograft.** The proteasome inhibitor bortezomib/Velcade has shown efficacy for the treatment of multiple myeloma as well as other hematologic and solid tumors (37, 38). Our observation that CRC cancer cells, like multiple myeloma, exhibit enhanced sensitivity to proteasome inhibitor-induced apoptosis *in vitro*

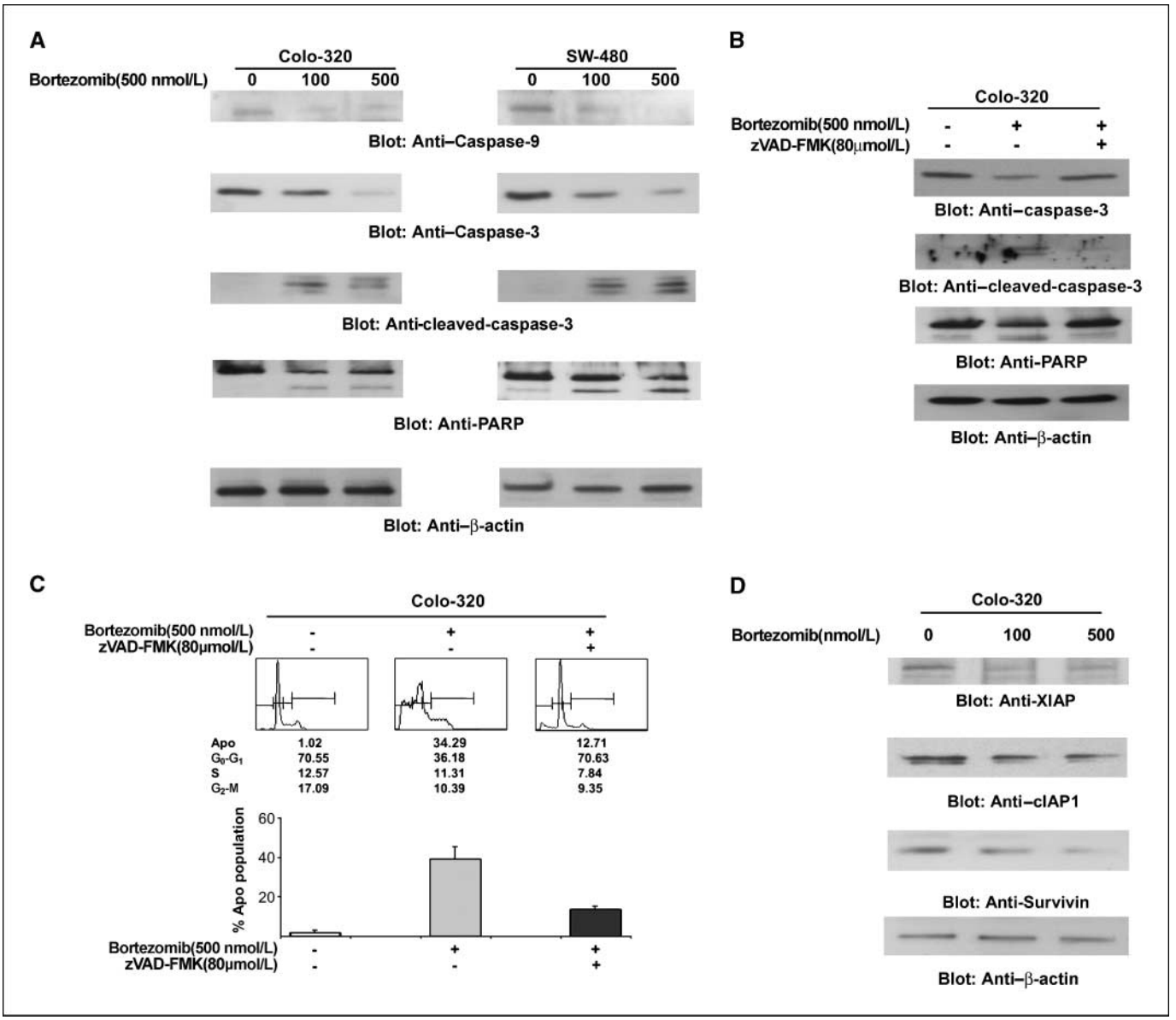

Figure 4. Activation of caspase-9 and caspase-3, and cleavage of PARP induced by bortezomib treatment in CRC cells. *A,* caspase-9, caspase-3, and PARP cleavage following bortezomib treatment. Colo320 and SW480 cells were treated with and without 100 and 500 nmol/L bortezomib for 48 h. Cells were lysed and 20 μg protein were separated by SDS-PAGE, transferred to PVDF membrane, and immunoblotted with antibodies against pro–caspase-9, pro–caspase-3, cleaved caspase-3, PARP, and β-actin. *B,* effect of z-VAD-fmk on bortezomib-induced activation of caspase-3 and cleavage of PARP. Colo320 cells were pretreated with either 80 μmol/L z-VAD/fmk for 2 h and subsequently treated with 500 nmol/L of bortezomib for 48 h. Cells were lysed and 20 μg protein were separated by SDS-PAGE, transferred to PVDF membrane, and immunoblotted with antibodies against pro–caspase-3, cleaved caspase-3, PARP, and β-actin. *C,* effect of z-VAD/fmk on bortezomib-induced apoptosis in CRC cells. Colo320 cells were pretreated with 80 μmol/L z-VAD/fmk for 2 h and subsequently treated with 500 nmol/L bortezomib, and apoptosis was measured by propidium iodide staining. *Columns,* mean of three independent experiments; *bars,* SD. *D,* bortezomib-induced down-regulation of XIAP, cIAP1, and survivin expression. Colo320 cells were treated with and without 100 and 500 nmol/L bortezomib for 48 h. Cells were lysed and equal amounts of proteins were separated on SDS-PAGE, transferred to PVDF membrane, and immunoblotted with antibodies against XIAP, cIAP1, survivin, and β-actin as indicated.

suggests the potential for therapeutic responses to treatment of colon cancer with proteasome inhibitors *in vivo*. Therefore, the ability of proteasome inhibitor bortezomib to inhibit CRC tumor growth was examined with a mouse xenograft model of CRC cancer. NUDE mice were inoculated s.c. in the right abdominal quadrant with 5 million Colo320 cells. After 1 week, mice were randomly assigned in two groups. Mice were then treated with bortezomib treatment group (1 mg/kg; $n = 5$) or 0.9% normal saline-treated control groups ($n = 5$) and treated by i.p. injection twice weekly. After 4 weeks of treatment, mice were sacrificed and tumors were collected. As shown in Fig. 5*A*, bortezomib treatment causes a time-dependent regression of Colo320-xenograft tumor in mice compared with vehicle-treated mice. The regression reached significance ($P < 0.05$) at the end of 4th week of treatment by bortezomib. A significant reduction in tumor weight (Fig. 5*B*) was observed in mice treated with bortezomib versus the control group ($P < 0.05$). Additionally, images of tumor before and after necropsy showed that bortezomib treatment resulted in shrinkage of tumor size (Fig. 5*C*). Because our *in vitro* data showed that bortezomib treatment down-regulated SKP2 and subsequently induced the expression of p27Kip1 in Colo320 cell line, we tested whether proteasome inhibition *in vivo* altered the expression of these proteins. We analyzed the SKP2 and p27Kip1 level in primary tumors derived from vehicle-treated mice and tumors treated with bortezomib mice by Western blot analysis. As shown in Fig. 5*D*, the level of SKP2 was markedly decreased in mice treated with bortezomib compared with vehicle-treated mice; on the other hand, the level of p27Kip1 was increased. Densitometry analysis indicated that the expression of SKP2 was significantly ($P < 0.05$) decreased whereas the expression of p27Kip1 was significantly increased (data not shown). It is also worthy to note that animal treated with proteasome inhibitors did not exhibit weight loss.

Discussion

Recent studies have clearly shown that SKP2 play an essential role in degradation of p27Kip1 (39). SKP2 protein enables efficient transfer of ubiquitin of p27Kip1, resulting in rapid proteasome-mediated degradation (9). Previous studies using purified extract from primary colon cancer tissue suggested that increased degradation of p27Kip1 by SKP2-dependent mechanism correlated with increased aggressiveness of the respective tumor. The interaction between these proteins was evident in a significant proportion of the study tumor samples, whereby the expression of

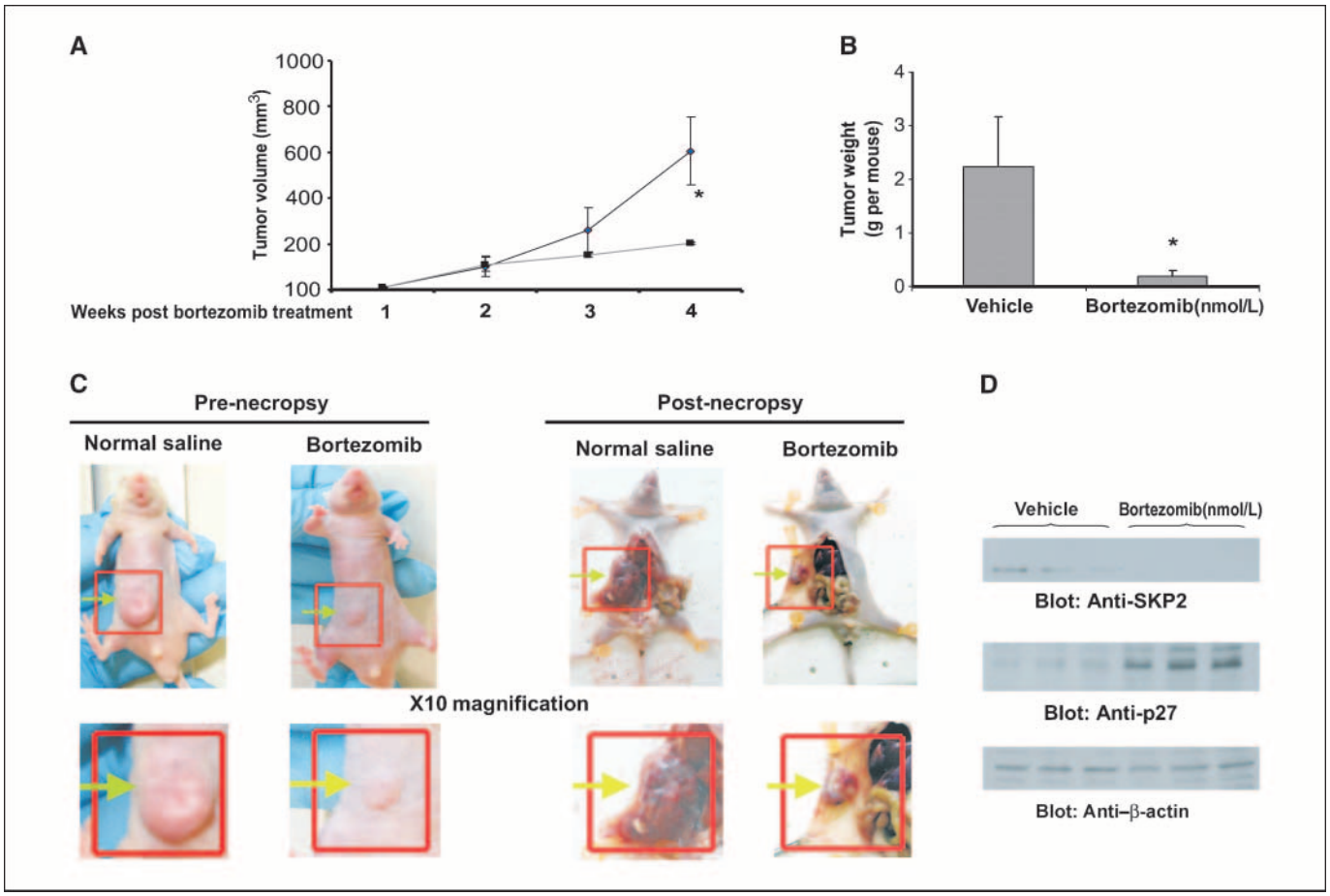

Figure 5. Bortezomib treatment inhibits growth of Colo320 xenograft and down-regulates SKP2 and increases levels of p27Kip1 *in vivo*. NUDE mice at 6 wk of age were injected i.p. with 5×10^6 Colo320 cells. After 1 wk, mice were treated with bortezomib at 1 mg/kg/dose or with 5% DMSO in PBS as a vehicle control. *A,* inhibition of Colo320 tumor growth by bortezomib. The volume of each tumor was measured every week after the start of treatment. The average ($n = 5$) tumor volume in vehicle-treated control mice and treated with bortezomib was plotted. *, $P < 0.05$. *B,* after 4 wk of treatment, mice were sacrificed and tumor weights were measured. *, $P < 0.05$ compared with vehicle-treated mice by Student's t test. *C,* representative tumor images of vehicle- and bortezomib-treated mice before and after necropsy. *Bottom,* images with ×10 magnification. *D,* whole-cell homogenates of individual tumor were prepared and Western blot analyses of SKP2, p27Kip1, and actin were carried out as described in Materials and Methods.

SKP2 was inversely associated with p27Kip1 protein levels (40). We therefore determined the role of both SKP2 and p27Kip1 as prognostic markers and found that those CRC that exhibit deregulation of SKP2 and p27Kip1, i.e., high level of SKP2 and low level of p27Kip1, have decreased overall survival. These clinical data as well as recent findings in cell lines and mice that suggest a potential role of SKP2 mediated p27Kip1 turnover have increased tendency of intestinal tumors to progress to a more malignant state (41). Altogether, these findings have prompted us in analyzing p27Kip1 regulation in CRC cell lines. Interestingly, we observed that CRC cell lines that displayed lower levels of p27Kip1 are showing increased level of SKP2. Proteasome inhibitors have been shown to stabilize a multiple number of cellular proteins, initially inducing arrest at G_2-M transition and ultimately leading to programmed cell death. Our data showed that bortezomib treatment of CRC cells down-regulated the expression of SKP2 with reciprocal up-regulation of p27Kip1, a well-known target of proteasome (42). Inhibition of SKP2 expression by specific SKP-2–siRNA increased p27Kip1 levels strongly, suggesting that bortezomib-mediated down-regulation of SKP2 and up-regulation p27Kip1 likely play significant roles in the induction of apoptosis in CRC cell lines. Apoptosis is a multistep process and increasing numbers of genes that are involved in the control or execution of apoptosis have been identified (43). Our study show that proteasomal inhibition by bortezomib in CRC cells caused apoptosis via activation of caspase-8 and truncation of BID that translocates to the mitochondrial membrane, allowing activation of proapoptotic proteins and release of cytochrome *c* into the cytosol. Released cytochrome *c* results in the formation apoptosome by interaction with apaf1 and caspase-9, leading to the activation of caspase-3, eventually resulting in cleavage of PARP in apoptotic cells, a hallmark of apoptosis by various antitumor agents (44). Furthermore, pretreatment of CRC cells with a broad-spectrum caspase inhibitor abrogated the bortezomib-induced apoptosis. These data suggest that inhibition of ubiquitin-proteasome in CRC induced apoptosis via caspase-cascade activation. Our *in vivo* studies further validate our hypothesis that treatment of mice bearing palpable CRC xenograft with bortezomib cause retarded tumor growth via down-regulation of SKP2 and increased level of P27Kip1 consistent with the *in vitro* effect of the proteasome inhibitors.

Bortezomib represent a novel class of myeloma therapy; several studies have shown the efficacy of the proteasome inhibitor bortezomib in variety of tumor cell lines and its synergistic antitumor activity has been shown in combination with other chemotherapy (45–47). Previous studies have shown that proteasome inhibitors induce up-regulation of tumor suppressor genes *p21* and *p27* via inhibition of other survival proteins, including nuclear factor-κB (7). Furthermore, bortezomib treatment showed synergistic antiproliferative and proapoptotic effects when combined with mitogen-activated protein kinase and EFGR inhibitor in *in vitro* studies (48, 49). Our *in vitro* data confirm the sensitivity of CRC cells to proteasomal inhibition. Furthermore, the apoptotic response is significantly enhanced after combination treatment with 5-fluorouracil and bortezomib. These data suggest that proteasome inhibitors may be new candidate chemotherapeutic agents for CRC treatment alone or in combination with other conventional chemotherapeutic agents.

Together, our results establish that the SKP2 ubiquitin-proteasome plays a role in the growth and survival of CRC cells. Down-regulation of SKP2 expression leads to accumulation and stabilization of p27Kip1, leading to the induction of apoptosis in CRC cells through release of cytochrome *c* from the mitochondria and activation of downstream caspases. In addition, CRC subgroup of patients with high SKP2 expression and low level of p27Kip1 show a poor overall survival. These studies may have important implications for future preclinical and clinical studies in CRC. Indeed, they may pave the way for investigations aimed at determining the usefulness of a novel strategy for treating CRC with inhibitors of proteasome pathways, either alone or in combination with other agents.

Acknowledgments

Received 11/6/2007; revised 1/18/2008; accepted 2/15/2008.

We thank Sriraman Devarajan for statistical analysis; Shakaib Siddiqui for data entry; and Azadali Moorji, Saeeda Omer Ahmed, Valerie Atizado, Hassan Al-Dossari, and Valorie Balde for technical assistance.

References

1. Douillard JY, Cunningham D, Roth AD, et al. Irinotecan combined with fluorouracil compared with fluorouracil alone as first-line treatment for metastatic colorectal cancer: a multicentre randomised trial. Lancet 2000;355:1041–7.
2. Khamly K, Jefford M, Michael M, et al. Beyond 5-fluorouracil: new horizons in systemic therapy for advanced colorectal cancer. Expert Opin Investig Drugs 2005;14:607–28.
3. Cunningham D, Humblet Y, Siena S, et al. Cetuximab monotherapy and cetuximab plus irinotecan in irinotecan-refractory metastatic colorectal cancer. N Engl J Med 2004;351:337–45.
4. Ciechanover A. The ubiquitin-proteasome proteolytic pathway. Cell 1994;79:13–21.
5. Ovaa H, Kessler BM, Rolen U, et al. Activity-based ubiquitin-specific protease (USP) profiling of virus-infected and malignant human cells. Proc Natl Acad Sci U S A 2004;101:2253–8.
6. Goldberg AL. Functions of the proteasome: the lysis at the end of the tunnel. Science 1995;268:522–3.
7. Cusack JC, Jr., Liu R, Xia L, et al. NPI-0052 enhances tumoricidal response to conventional cancer therapy in a colon cancer model. Clin Cancer Res 2006;12:6758–64.
8. McDade TP, Perugini RA, Vittimberga FJ, Jr., et al. Ubiquitin-proteasome inhibition enhances apoptosis of human pancreatic cancer cells. Surgery 1999;126:371–7.
9. Carrano AC, Eytan E, Hershko A, et al. SKP2 is required for ubiquitin-mediated degradation of the CDK inhibitor p27. Nat Cell Biol 1999;1:193–9.
10. Sutterluty H, Chatelain E, Marti A, et al. p45SKP2 promotes p27Kip1 degradation and induces S phase in quiescent cells. Nat Cell Biol 1999;1:207–14.
11. Tsvetkov LM, Yeh KH, Lee SJ, et al. p27(Kip1) ubiquitination and degradation is regulated by the SCF(Skp2) complex through phosphorylated Thr187 in p27. Curr Biol 1999;9:661–4.
12. Lwin T, Hazlehurst LA, Dessureault S, et al. Cell adhesion induces p27Kip1-associated cell-cycle arrest through down-regulation of the SCFSkp2 ubiquitin ligase pathway in mantle cell and other non-Hodgkin's B-cell lymphomas. Blood 2007;110:1631–8.
13. Signoretti S, Di Marcotullio L, Richardson A, et al. Oncogenic role of the ubiquitin ligase subunit Skp2 in human breast cancer. J Clin Invest 2002;110:633–41.
14. Hershko D, Bornstein G, Ben-Izhak O, et al. Inverse relation between levels of p27(Kip1) and of its ubiquitin ligase subunit Skp2 in colorectal carcinomas. Cancer 2001;91:1745–51.
15. Yang G, Ayala G, De Marzo A, et al. Thompson TC, Harper JW. Elevated Skp2 protein expression in human prostate cancer: association with loss of the cyclin-dependent kinase inhibitor p27 and PTEN and with reduced recurrence-free survival. Clin Cancer Res 2002;8:3419–26.
16. Soligo D, Servida F, Delia D, et al. The apoptogenic response of human myeloid leukaemia cell lines and of normal and malignant haematopoietic progenitor cells to the proteasome inhibitor PSI. Br J Haematol 2001;113:126–35.
17. Orlowski RZ, Eswara JR, Lafond-Walker A, et al. Tumor growth inhibition induced in a murine model of human Burkitt's lymphoma by a proteasome inhibitor. Cancer Res 1998;58:4342–8.
18. Thornberry NA, Lazebnik Y. Caspases: enemies within. Science 1998;281:1312–6.
19. Adams J. Proteasome inhibition in cancer: development of PS-341. Semin Oncol 2001;28:613–9.
20. Richardson PG. Bortezomib: a novel therapy approved for multiple myeloma. Clin Adv Hematol Oncol 2003;1:596–600.
21. Bazzaro M, Lee MK, Zoso A, et al. Ubiquitin-proteasome system stress sensitizes ovarian cancer to proteasome inhibitor-induced apoptosis. Cancer Res 2006;66:3754–63.
22. Hussain AR, Al-Rasheed M, Manogaran PS, et al.

Curcumin induces apoptosis via inhibition of PI3'-kinase/AKT pathway in acute T cell leukemias. Apoptosis 2006;11:245–54.
23. Hussain AR, Al-Jomah NA, Siraj AK, et al. Sanguinarine-dependent induction of apoptosis in primary effusion lymphoma cells. Cancer Res 2007;67:3888–97.
24. Uddin S, Ah-Kang J, Ulaszek J, et al. Differentiation stage-specific activation of p38 mitogen-activated protein kinase isoforms in primary human erythroid cells. Proc Natl Acad Sci U S A 2004;101:147–52.
25. Uddin S, Hussain AR, Al-Hussein KA, et al. Inhibition of phosphatidylinositol 3'-kinase/AKT signaling promotes apoptosis of primary effusion lymphoma cells. Clin Cancer Res 2005;11:3102–8.
26. Uddin S, Hussain AR, Al-Hussein KA, et al. Role of phosphatidylinositol 3'-kinase/AKT pathway in diffuse large B-cell lymphoma survival. Blood 2006;108:4178–86.
27. Bavi P, Jehan Z, Atizado V, et al. Prevalence of fragile histidine triad expression in tumors from Saudi Arabia: a tissue microarray analysis. Cancer Epidemiol Biomarkers Prev 2006;15:1708–18.
28. Shapira M, Ben-Izhak O, Bishara B, et al. Alterations in the expression of the cell cycle regulatory protein cyclin kinase subunit 1 in colorectal carcinoma. Cancer 2004;8:1615–21.
29. Levkau B, Koyama H, Raines EW, et al. Cleavage of p21Cip1/Waf1 and p27Kip1 mediates apoptosis in endothelial cells through activation of Cdk2: role of a caspase cascade. Mol Cell 1998;1:553–63.
30. Coulombe P, Rodier G, Bonneil E, et al. N-terminal ubiquitination of extracellular signal-regulated kinase 3 and p21 directs their degradation by the proteasome. Mol Cell Biol 2004;24:6140–50.
31. Pagano M, Tam SW, Theodoras AM, et al. Role of the ubiquitin-proteasome pathway in regulating abundance of the cyclin-dependent kinase inhibitor p27. Science 1995;269:682–5.
32. Adams J, Palombella VJ, Sausville EA, et al. Proteasome inhibitors: a novel class of potent and effective antitumor agents. Cancer Res 1999;59:2615–22.
33. Dulic V, Stein GH, Far DF, et al. Nuclear accumulation of p21Cip1 at the onset of mitosis: a role at the G2-M-phase transition. Mol Cell Biol 1998;18:546–57.
34. Hideshima T, Richardson P, Chauhan D, et al. The proteasome inhibitor PS-341 inhibits growth, induces apoptosis, and overcomes drug resistance in human multiple myeloma cells. Cancer Res 2001;61:3071–6.
35. Chen F, Harrison LE. Ciglitazone-induced cellular anti-proliferation increases p27kip1 protein levels through both increased transcriptional activity and inhibition of proteasome degradation. Cell Signal 2005;17:809–16.
36. Dan HC, Sun M, Kaneko S, et al. Akt phosphorylation and stabilization of X-linked inhibitor of apoptosis protein (XIAP). J Biol Chem 2004;279:5405–12.
37. Gardner RC, Assinder SJ, Christie G, et al. Characterization of peptidyl boronic acid inhibitors of mammalian 20S and 26S proteasomes and their inhibition of proteasomes in cultured cells. Biochem J 2000;2:447–54.
38. Rivett AJ, Gardner RC. Proteasome inhibitors: from *in vitro* uses to clinical trials. J Pept Sci 2000;6:478–88.
39. Ganoth D, Bornstein G, Ko TK, et al. The cell-cycle regulatory protein Cks1 is required for SCF (Skp2)-mediated ubiquitinylation of p27. Nat Cell Biol 2001;3:321–4.
40. Chiappetta G, De Marco C, Quintiero A, et al. Overexpression of the S-phase kinase-associated protein 2 in thyroid cancer. Endocr Relat Cancer 2007;14:405–20.
41. Timmerbeul I, Garrett-Engele CM, Kossatz U, et al. Testing the importance of p27 degradation by the SCFskp2 pathway in murine models of lung and colon cancer. Proc Natl Acad Sci U S A 2006;38:14009–14.
42. Mani A, Gelmann EP. The ubiquitin-proteasome pathway and its role in cancer. The ubiquitin-proteasome pathway and its role in cancer. J Clin Oncol 2005;23:4776–89.
43. Gastman BR. Apoptosis and its clinical impact. Head Neck 2001;23:409–25.
44. Nunez G, Benedict MA, Hu Y, et al. Caspases: the proteases of the apoptotic pathway. Oncogene 1998;24:3237–45.
45. Richardson P. Clinical update: proteasome inhibitors in hematologic malignancies. Cancer Treat Rev 2003;29 Suppl 1:33–9.
46. Jagannath S, Barlogie B, Berenson J, et al. A phase 2 study of two doses of bortezomib in relapsed or refractory myeloma. Br J Haematol 2004;127:165–72.
47. Frankel A, Man S, Elliott P, et al. Lack of multicellular drug resistance observed in human ovarian and prostate carcinoma treated with the proteasome inhibitor PS-341. Clin Cancer Res 2000;6:3719–28.
48. Navas TA, Nguyen AN, Hideshima T, et al. Inhibition of p38α MAPK enhances proteasome inhibitor-induced apoptosis of myeloma cells by modulating Hsp27, Bcl-X(L), Mcl-1 and p53 levels *in vitro* and inhibits tumor growth *in vivo*. Leukemia 2006;20:1017–27.
49. An J, Rettig MB. Epidermal growth factor receptor inhibition sensitizes renal cell carcinoma cells to the cytotoxic effects of bortezomib. Mol Cancer Ther 2007;6:61–9.

Bortezomib (Velcade) Induces p27Kip1 Expression through S-Phase Kinase Protein 2 Degradation in Colorectal Cancer

Shahab Uddin, Maqbool Ahmed, Prashant Bavi, et al.

Cancer Res 2008;68:3379-3388.